

Journal of
**Applied
Crystallography**

ISSN 0021-8898

Editor: **Gernot Kosterz**

High-resolution synchrotron radiation studies on natural and thermally annealed scleractinian coral biominerals

J. Stolarski, R. Przeniosło, M. Mazur and M. Brunelli

Copyright © International Union of Crystallography

Author(s) of this paper may load this reprint on their own web site provided that this cover page is retained. Republication of this article or its storage in electronic databases or the like is not permitted without prior permission in writing from the IUCr.

High-resolution synchrotron radiation studies on natural and thermally annealed scleractinian coral biominerals

J. Stolarski,^{a*} R. Przeniosło,^b M. Mazur^c and M. Brunelli^d^aInstitute of Paleobiology, Polish Academy of Sciences, Twarda 51/55, PL-00-818 Warsaw, Poland,^bInstitute of Experimental Physics, Warsaw University, Hoża 69, PL-00-681 Warsaw, Poland,^cDepartment of Chemistry, Laboratory of Electrochemistry, Warsaw University, Pasteura 1, PL-02-093 Warsaw, Poland, and ^dEuropean Synchrotron Radiation Facility, BP 220, F-38043 Grenoble Cedex, France. Correspondence e-mail: stolacy@twarda.pan.pl

The structural phase transition from aragonite to calcite in biogenic samples extracted from the skeletons of selected scleractinian corals has been studied by synchrotron radiation diffraction. Biogenic aragonite samples were extracted *en bloc* without pulverization from two ecologically different scleractinian taxa: *Desmophyllum* (deep-water, solitary and azooxanthellate) and *Favia* (shallow-water, colonial, zooxanthellate). It was found that natural (not pulverized) samples contribute to narrow Bragg peaks with $\Delta d/d$ values as low as 1×10^{-3} , which allows the exploitation of the high resolution of synchrotron radiation diffraction. A precise determination of the lattice parameters of biogenic scleractinian coral aragonite shows the same type of changes of the *a*, *b*, *c* lattice parameter ratios as that reported for aragonite extracted from other invertebrates [Pokroy, Quintana, Caspi, Berner & Zolotoyabko (2004). *Nat. Mater.* **3**, 900–902]. It is believed that the crystal structure of biogenic samples is influenced by interactions with organic molecules that are initially present in the biomineralization hydrogel. The calcite phase obtained by annealing the coral samples has a considerably different unit-cell volume and lattice parameter ratio *c/a* as compared with reference geological calcite and annealed synthetic aragonite. The internal strain in the calcite structure obtained by thermal annealing of the biomineral samples is about two times larger than that found in the natural aragonite structure. This effect is observed despite slow heating and cooling of the sample.

© 2007 International Union of Crystallography
Printed in Singapore – all rights reserved

1. Introduction

Skeletal structures of organisms recently became the object of broad interdisciplinary studies as their functionally optimized properties arouse inspiration for rapidly growing interest in nanotechnology and biomaterial research domains (Jelinski, 1999). Various skeletal biominerals are the target of studies, including calcium carbonate compounds that occur most widely in nature. For example, mollusk nacre and skeletons of scleractinian corals (especially reef-builders) are known for their mechanical strength, which is partly attributed to their composite structure; the crystallographically ordered biomineral nano- and micro-components are closely associated with the organic molecules and form complex hierarchical structures (*e.g.* Grégoire, 1967; Mutvei, 1969, 1979; Currey & Kohn, 1976; Cuif & Dauphin, 2005a; Rousseau *et al.*, 2005). Notably, the composite structure of the scleractinian coral skeleton was only recently elucidated, challenging the long-kept concept of their purely crystalline CaCO₃ (aragonite) composition (Cuif

et al., 1997; Stolarski, 2003; Cuif & Dauphin, 2005b; Stolarski & Mazur, 2005). The occurrence of the intraskeletal organic components of coral skeletons has been assessed in the bulk samples by thermogravimetric (Cuif *et al.*, 2004; Stolarski & Mazur, 2005), chromatographic (Dauphin, 2001) and spectroscopic (Cuif & Dauphin, 1998) methods, whereas their spatial distribution pattern has been studied by histological staining (Gautret *et al.*, 2000; Stolarski, 2003) and synchrotron radiation (SR) mapping techniques (Cuif *et al.*, 2003).

Although the amount of the organic phase embedded in the coral skeleton is estimated to be in the range 0.1–2.5% (Wainwright, 1963; Cuif *et al.*, 2004), the resulting composite mineral (aragonite)–organic material exhibits significantly different properties as compared with synthetically produced CaCO₃. Recent high-resolution SR studies have shown that aragonite in the mollusk skeleton has an *ab/c* lattice parameter ratio different from that of geological origin (Pokroy *et al.*, 2004; Pokroy, Fitch, Lee *et al.*, 2006). Numerous biogenic aragonite samples show a systematic elongation of the lattice

constants a and c and contraction of the lattice constant b as compared with reference geological aragonite. This anisotropic elongation is probably due to intercalation of organic molecules into the crystallographic lattice during the biomineralization process (Pokroy, Fitch, Lee *et al.*, 2006). It has also been shown that the aragonite–calcite phase transformation of the scleractinian coral biomineral was initiated and completed at lower temperature than for aragonite that formed in an inorganic environment (*e.g.* Yoshika & Kitano, 1985; Ganteaume *et al.*, 1990; Passe-Coutrin *et al.*, 1995; Fricain *et al.*, 2002). Recent research on the aragonite–calcite phase transition in synthetic aragonite (Lucas *et al.*, 1999) and coral biomineral (Vongsavat *et al.*, 2006) has been focused on changes of elastic coefficients and the content of paramagnetic Mn^{2+} and free radicals in thermally treated samples. However, so far, X-ray diffraction studies of coral $CaCO_3$ biominerals have been performed on powdered samples only (Pokroy, Fitch, Lee *et al.*, 2006; Vongsavat *et al.*, 2006); thus their crystallographic properties might have been changed during the pulverization process. In addition, Fricain *et al.* (2002) have shown that the complete aragonite–calcite phase transition in coral samples extracted *en bloc* requires annealing times shorter than the transformation in pulverized coral samples.

In this paper we report for the first time a high-resolution synchrotron radiation study of natural and annealed biomineral samples extracted *en bloc* from the skeleton of modern scleractinian corals

2. Materials and methods

2.1. Synthetic aragonite

Synthetic aragonite was precipitated by using the following procedure. An aqueous solution (20 ml) containing 0.1 M $CaCl_2$ (Sigma-Aldrich, > 96%) and 0.06 M $MgCl_2$ (POCh, reagent grade) was added slowly to a boiling 0.1 M Na_2CO_3 solution (20 ml) (Sigma-Aldrich, > 99.5%). The precipitate was then separated by filtration and carefully rinsed with distilled water (Milli-Q quality). The resulting aragonite was further dried at 383 K for 1 h (Lucas *et al.*, 1999). After drying, the precipitate was cooled slowly to room temperature.

2.2. Biomineral sample preparation

Samples of biomineral were extracted from extant scleractinian corals representing two ecologically distinct groups: (1) *Favia stelligera* (Dana, 1846), representative of colonial, shallow-water and zooxanthellate corals (collection site Lizard Island, Great Barrier Reef, Pacific Ocean, 5–10 m; sample number ZPAL V.31/1), and (2) *Desmophyllum dianthus* (Esper, 1794), solitary, deep-water, azooxanthellate coral (collection site off Chile, station 51052, Pacific Ocean, 51°52.0'S/73°41.0'W, 636 m; sample number ZPAL H.25/5-Car). Two distinctly different coral species were selected to test whether the phase transformation differs between these biominerals, whose intraskeletal organic components show significant biochemical divergence (Cuif *et al.*, 1999). For

brevity, in the text the samples of *Favia stelligera* are referred to as *Favia* and those of *Desmophyllum dianthus* as *Desmophyllum*. All specimens are housed in the Institute of Paleobiology, Polish Academy of Sciences, Warsaw (ZPAL).

Sampling regions, devoid of boring traces by endolithic organisms that would contaminate the biomineral, were preliminarily selected by using a Nikon SMZ800 stereoscopic zoom microscope. Five samples chosen from the external wall of *Desmophyllum*, and 2–3 corallites constituting a part of the colony of *Favia*, were cut by means of a diamond saw (Dremel 545 Diamond Wheel). Small blocks of $ca\ 10 \times 10 \times 5$ mm were polished with diamond powder 1200 Grit and aluminium oxide (Buehler TOPOL 3 final polishing suspension with particle size 0.25 μm). After polishing, the sections were rinsed with distilled water and washed in an ultrasonic cleaner for 10 s.

To visualize the relief of polished biomineral samples (*Favia*, *Desmophyllum*) that were examined by scanning electron microscopy (SEM; Philips XL 20) they were exposed for $ca\ 20$ s to 0.1% formic acid solution (POCh, 85%). Formic acid is known to dissolve not only mineral but also organic components (Waite & Andersen, 1980); therefore etching of the samples yields a distinct negative relief corresponding to regions (Figs. 1 and 2) enriched in organic content (see also Stolarski, 2003). The etched samples were rinsed with distilled water and air-dried. After drying, the samples were mounted on stubs with double-sided adhesive tape and sputter-coated with conductive platinum film.

2.3. Thermal treatment

Part of the samples (synthetic aragonite and biomineral ones) were thermally annealed to produce transformation of aragonite to calcite. The procedure involved heating of the samples in air at linear gradient (10 K min^{-1}) from ambient 293 K to 773 K. The sample was kept at 773 K for 1 h and then allowed to cool slowly for $ca\ 12$ h. The experimental details were adjusted on the basis of our previous thermogravimetric measurements (Stolarski & Mazur, 2005). Under these conditions all aragonite is transformed to calcite, while further decomposition of the mineral to CaO is hindered. Annealed biomineral samples remain solid and preserve the original macroscopic details of the coral skeleton. The visible difference between annealed and natural biomineral samples is their color; after thermal treatment the originally white–yellow skeleton changes into a white–gray one that most likely is associated with the decomposition of the intraskeletal organic components (Cuif *et al.*, 2004; Dauphin *et al.*, 2006).

2.4. High-resolution SR studies

High-resolution SR studies were performed at the ESRF beamline ID31 [for a description of the instrument see Fitch (2004)]. The coral samples, extracted *en bloc* from the skeleton and showing approximately parallelepiped shape of dimensions $8 \times 4 \times 1$ mm, were mounted directly in transmission mode in the SR beam. The coral sample was immobile during the measurements. In this study we used different SR wavelengths because the examined mineral compounds do not

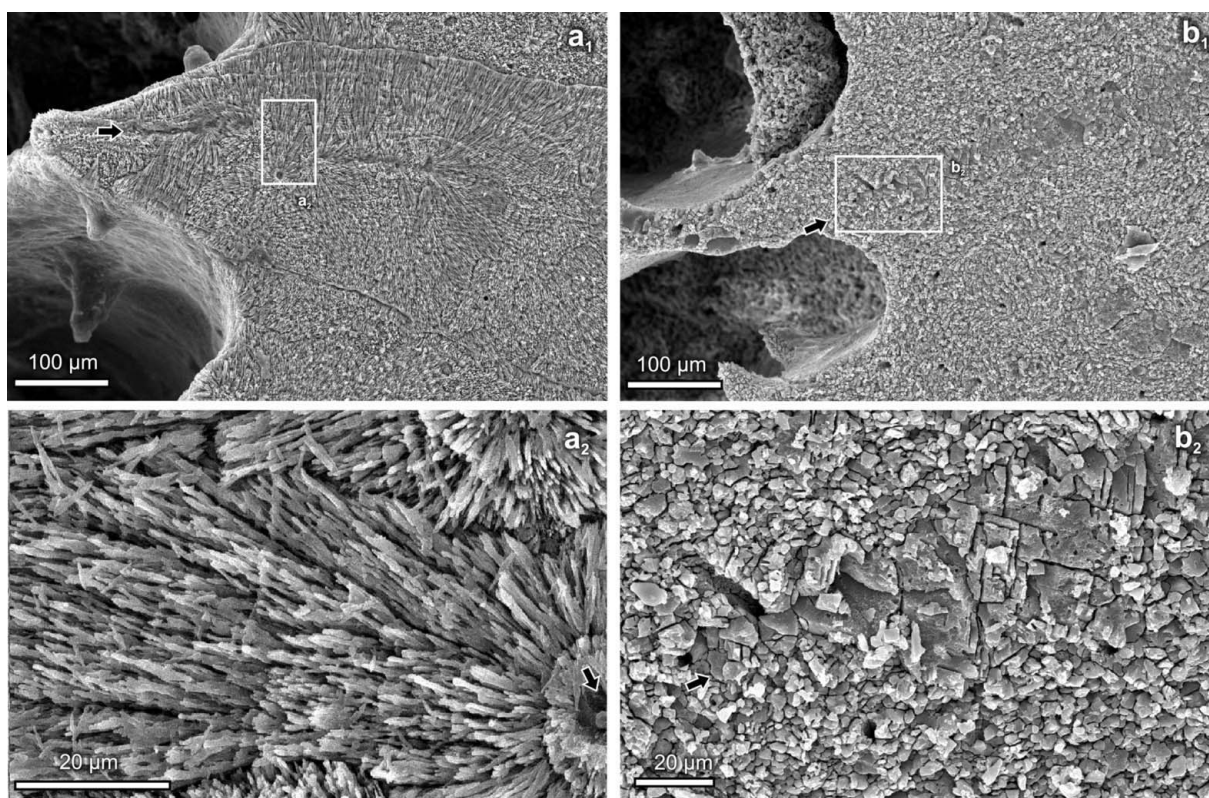


Figure 1

Sample of *Favia* (*F. stelligera*, ZPAL.V.31/1) (a) before and (b) after the annealing treatment at 773 K, at two SEM magnifications (a_1 , b_1) and (a_2 , b_2). (a_1 , a_2) Polished and etched (formic acid, 1%, 20 s) transverse section of septal and wall skeleton with aragonite fibers radiating from CRAs. Black arrows indicate the negative etching relief of CRA regions that are particularly enriched in organic components (see Stolarski, 2003). (b_1 , b_2) The same skeleton annealed; the fibrous skeletal texture is replaced by irregularly arranged calcite grains. The original position of the CRA is indicated by larger calcite grains.

require any specific value of wavelength for diffraction experiments and equally good data sets (in terms of statistics and resolution) can be recorded in the reported range of energies. Therefore X-ray powder diffraction experiments were carried out at different times at the ID31 beamline without changing the existing setup.

SR diffraction measurements of natural and annealed *Desmophyllum* samples were performed at a wavelength of $\lambda = 0.40111$ (1) Å for scattering angles $2 \leq 2\theta \leq 26^\circ$. SR diffraction measurements of natural and annealed *Favia* were performed at $\lambda = 0.30001$ (2) Å for scattering angles $2 \leq 2\theta \leq 20^\circ$. SR measurements were also performed for a polycrystalline (powder) synthetic aragonite sample sealed in a 0.7 mm diameter borosilicate capillary. As-prepared and annealed synthetic aragonite samples were studied by SR diffraction at $\lambda = 1.25248$ (3) Å for scattering angles $2 \leq 2\theta \leq 82^\circ$.

The observed SR diffraction patterns were analyzed by the Rietveld method (Rietveld, 1969) with the use of the *FullProf* software (Rodriguez-Carvajal, 1993). The FWHM of the observed lines was analyzed by the Williamson–Hall method (Williamson & Hall, 1953). The instrumental resolution of the ID31 diffractometer was estimated from measurements with an LaB_6 standard.

3. Results

3.1. SEM microscopic observations

Synthetic and biogenic aragonite samples were examined by using SEM before and after the annealing process.

The synthetic aragonite precipitate consisted of aggregates (about 5–15 μm long, 2–5 μm in diameter) of acicular crystals, each about 0.4 μm in diameter. Elongated ‘aggregates’ are still recognizable in the annealed samples of synthetic CaCO_3 , although their regular fibrous structure is no longer recognizable. Rhombohedral calcite crystals also occur frequently in the annealed sample.

In polished and etched sections of the natural skeleton of *Favia* and *Desmophyllum* two main regions are recognizable, described in biological literature as calcification centers [or centers of rapid accretion (CRAs) or early mineralization zones] and fibers (thickening deposits) (see Cuif *et al.*, 2003; Stolarski, 2003). The calcification centers are greatly enriched in organic components and thus exhibit a strong negative relief in etched sections, whereas fibers, which contain less organic matter, show generally positive etching relief with some important exceptions; etching accentuates borders between bundles of fibers and their successive growth steps that are regularly distributed and dense in *Favia* (every

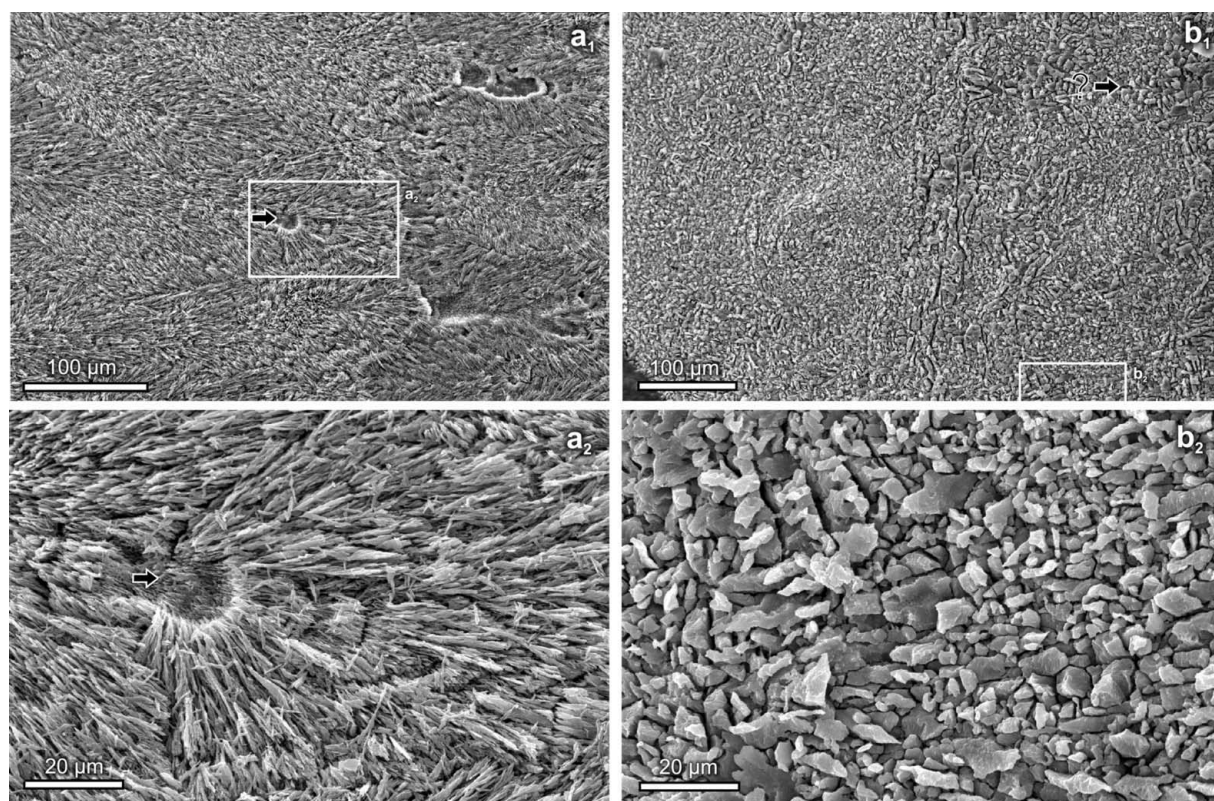


Figure 2

Sample of *Desmophyllum* (*D. dianthus*, ZPAL H.25/5-Car) (a) before and (b) after annealing treatment at 773 K, at two SEM magnifications (a_1 , b_1) and (a_2 , b_2). (a_1 , a_2) Polished and etched (formic acid, 1%, 20 s) wall skeleton with aragonite fibers radiating from CRAs (the black arrow indicates the negative etching relief of the CRA region that originally was enriched in organic components). (b_1 , b_2) The same skeleton annealed; the fibrous skeletal texture is replaced by irregularly arranged calcite grains. The possible original position of the CRA is indicated by a black arrow.

ca 3–5 μm ; Figs. 1 a_1 and 1 a_2) and less regular and more widely spaced in *Desmophyllum* (ca 10 μm ; Figs. 2 a_1 and 2 a_2). In both annealed samples, fibers are no longer recognizable (Fig. 1 b_1 , 1 b_2 , 2 b_1 and 2 b_2) and the etching relief of the originally fibrous parts shows small grains, typically 5–10 μm in diameter (Figs. 1 b_2 and 2 b_2). In *Favia*, grains are larger (ca 20 μm in diameter) and show a rhombohedral character in zones of the original positions of calcification centers (Fig. 1 b_2). In *Desmophyllum*, such a differentiation of grain sizes is less prominent (Fig. 2 b_1), although the examined samples also originally contained only sparsely distributed calcification centers (Fig. 2 a_1).

3.2. SR diffraction – Rietveld fits

The SR diffraction pattern of natural *Favia* shows Bragg peaks due to the aragonite structure (Pilati *et al.*, 1998; Jarosch & Heger, 1986; Caspi *et al.*, 2005) but also weak peaks due to the calcite structure (Maslen *et al.*, 1995). In the Rietveld analysis the aragonite and calcite structure models given by Caspi *et al.* (2005) and Maslen *et al.* (1995), respectively, were assumed. We refined the lattice constants and preserved the atomic positions and displacement parameters as they were given in the literature. The atomic coordinates could not be determined because of important texture effects observed on diffraction patterns measured in biomineral samples mounted

en bloc. The results of the Rietveld analysis are shown in Fig. 3. Agreement with the aragonite structure is good and the texture is weakly developed; the Bragg R factor $R_B = 8\%$. The estimated amount of calcite phase is 2 wt%. In order to compare our experimental results with the recent reference studies of geological aragonite (Caspi *et al.*, 2005) we show the enlarged doublet of 102 and 200 Bragg peaks in the inset in Fig. 3.

The SR diffraction pattern of natural *Desmophyllum* coral shows only Bragg peaks at positions corresponding to the aragonite diffraction pattern without any impurity phase contributions. The mineral phase of natural *Desmophyllum* is strongly textured. Rietveld analysis (not shown in the figure) yields a high value of the Bragg factor ($R_B = 35\%$).

The SR diffraction pattern of as-prepared synthetic aragonite shows broader peaks (with larger values of $\Delta d/d$) than the biogenic samples. In addition to aragonite Bragg peaks there are also some broad maxima located near the positions expected for peaks due to the calcite structure (Maslen *et al.*, 1995). The estimated amount of this impurity phase is about 20%. These broad contributions [possibly including some amorphous calcium carbonate phase (Ajikumar *et al.*, 2005)] have been excluded from further analysis. A Rietveld fit of the as-prepared synthetic aragonite gives $R_B = 14\%$, indicating some texture.

Table 1

Orthorhombic lattice parameters a , b , c (Å) and the unit-cell volume V (Å³) determined for different kinds of biogenic, geological and synthetic aragonite.

No.		a	b	c	V
Biogenic					
1	<i>Desmophyllum</i>	4.96499 (5)	7.96992 (8)	5.74892 (8)	227.488 (5)
2	<i>Favia</i>	4.96509 (2)	7.97226 (3)	5.75004 (2)	227.603 (2)
Geological					
3	Caspi <i>et al.</i> (2005)	4.96183 (1)	7.96914 (2)	5.74285 (2)	227.081 (2)
4	De Villiers (1970)	4.96140 (30)	7.96710 (40)	5.74040 (40)	226.906 (24)
Synthetic					
5	As-prepared	4.96053 (5)	7.96965 (4)	5.74293 (5)	227.174 (3)
6	Lucas <i>et al.</i> (1999)	4.96200 (40)	7.97000 (60)	5.74440 (80)	227.040 (40)

The refined lattice parameters of aragonite obtained from SR diffraction patterns of *Desmophyllum*, *Favia* and synthetic aragonite are compared with literature data in Table 1. Our results for synthetic as-prepared aragonite agree well with those of Lucas *et al.* (1999). The unit-cell volumes for biogenic samples are considerably larger than those for synthetic and geological samples. We tried to verify whether our biogenic aragonite samples show the same changes of the $a/b/c$ lattice parameter ratios as that reported by Pokroy, Fitch, Lee *et al.* (2006). In order to exclude the possibility of systematic errors due to wavelength calibration, the lattice parameter ratios are analyzed in Fig. 4. Our biogenic samples show the same kind of anisotropic elongation as reported by Pokroy, Fitch, Lee *et al.* (2006), where systematic deviations are reported for the lattice parameters with respect to the reference geological sample (Caspi *et al.*, 2005) with positive $\Delta a/a$ (ca 0.1%), negative $\Delta b/b$ (ca -0.05%) and positive $\Delta c/c$ (ca 0.15%) elongations. One can see in Fig. 4 that the lattice parameter ratios obtained for both biogenic samples differ from those of the reference geological and as-prepared synthetic aragonite.

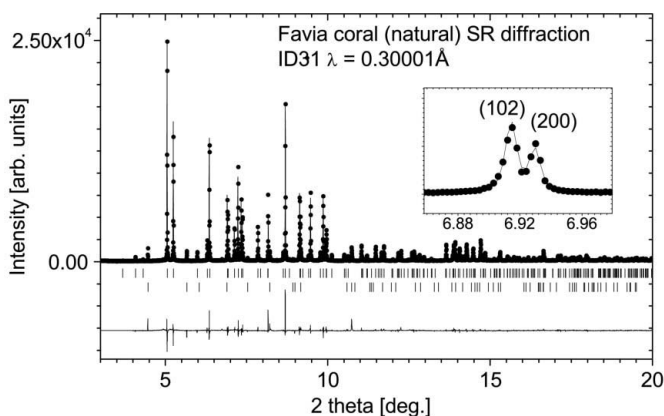


Figure 3

Results of the Rietveld refinement of the SR diffraction pattern of the mineral phase of natural *Favia*. Points denote measured data; the continuous line is the profile calculated by assuming the reference aragonite structure (Jarosch & Heger, 1986) and a small amount of calcite (Maslen *et al.*, 1995). The line below the pattern shows the difference between the measured and the calculated patterns. The upper and lower rows of ticks indicate the positions of the Bragg peaks due to the aragonite and calcite phases. The inset shows an enlarged part of the diffraction pattern with the 102 and 200 Bragg peaks.

Table 2

Hexagonal lattice parameters a , c (Å) and the unit-cell volume V (Å³) determined for different kinds calcite obtained from annealing biogenic *Desmophyllum* and *Favia* and as-prepared aragonite samples; the data are compared with literature values for synthetic calcite (Maslen *et al.*, 1995).

	a	c	ca	V
Biogenic				
<i>Desmophyllum</i>	4.98861 (4)	17.07870 (16)	3.4235	368.082 (6)
<i>Favia</i>	4.98911 (2)	17.07858 (8)	3.4232	368.153 (3)
Synthetic				
Annealed	4.98837 (4)	17.06862 (14)	3.4217	367.830 (6)
Maslen <i>et al.</i> (1995)	4.98800 (20)	17.06800 (20)	3.4218	367.761 (21)

Thus, our results confirm previous literature reports (Pokroy *et al.*, 2004; Pokroy, Fitch, Lee *et al.*, 2006).

The annealed samples of *Favia* and *Desmophyllum* also had parallelepiped shape (*en bloc*). The SR diffraction patterns of annealed *Favia*, *Desmophyllum* and as-prepared synthetic aragonite show exclusively Bragg peaks due to the calcite structure (Maslen *et al.*, 1995). The SR diffraction pattern of annealed synthetic aragonite shows weak, broad contributions near the calcite Bragg peaks (similar positions to the impurity phase contributions observed in the as-prepared synthetic aragonite). These weak contributions have also been excluded from the refinements. The results of the Rietveld fit for annealed *Favia* are shown in Fig. 5. There is some texture and

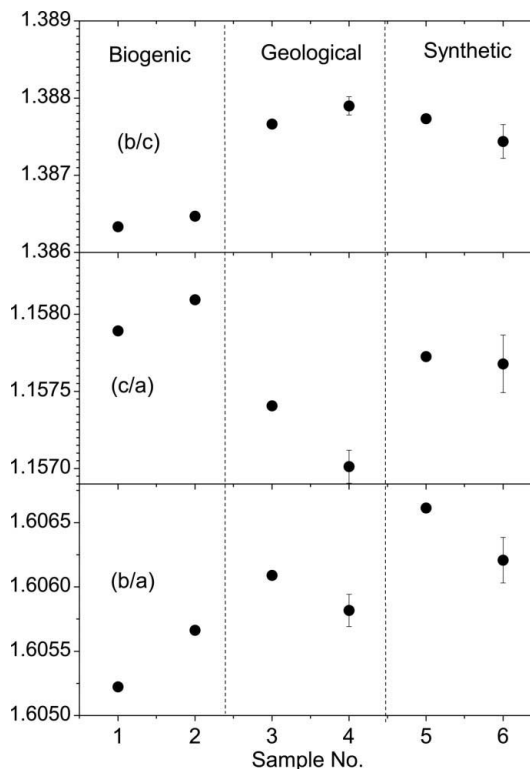
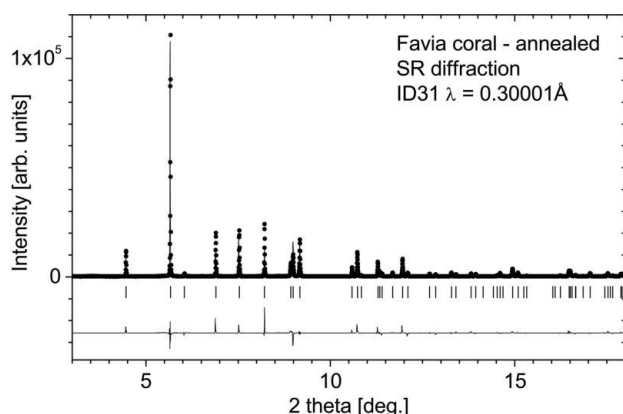


Figure 4

Orthorhombic lattice constant ratios b/c (upper), c/a (middle) and b/a (lower) determined from SR diffraction Rietveld analysis of aragonite samples. The sample numbers on the horizontal axis are defined in Table 1.


Figure 5

Results of the Rietveld refinement of the SR diffraction pattern of the mineral phase of natural *Favia* annealed at 773 K. The points denote measured data; the continuous line is the profile calculated by assuming the reference calcite structure (Maslen *et al.*, 1995). The line below the pattern shows the difference between the measured and the calculated patterns. The ticks indicate the positions of the Bragg peaks.

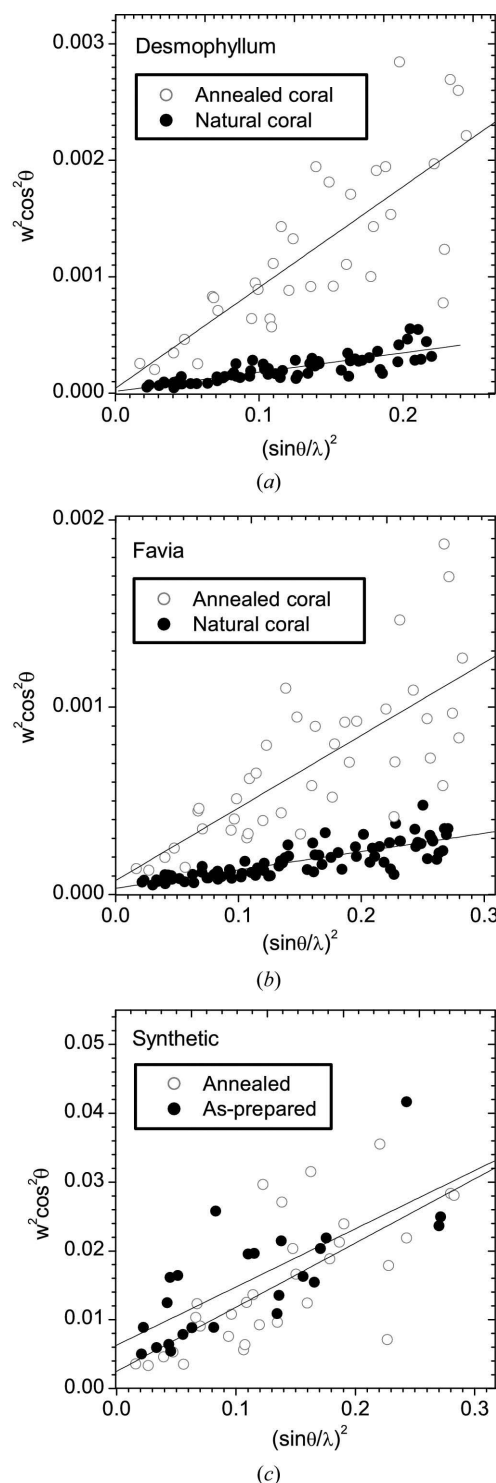
the Bragg R factors obtained for annealed samples of *Favia*, *Desmophyllum* and as-prepared synthetic aragonite are $R_B = 16, 8$ and 17%, respectively. The lattice parameters are shown in Table 2. The unit-cell volumes, V , and the c/a ratios of both biogenic samples are considerably different from the synthetic values. It can be concluded that the microstructure of biogenic aragonite influences the crystal structure of the calcite phase generated after annealing. Notably, a recent study of calcite biominerals (Pokroy, Fitch, Marin *et al.*, 2006) shows similar results, with c/a ratios varying between 3.4234 and 3.4258 for natural skeletons of five different mollusk species. Pokroy, Fitch, Marin *et al.* (2006) also report c/a values for synthetic and geological calcite of 3.4200 and 3.4195, respectively.

3.3. SR diffraction – microstrain

The Bragg peak broadening due to grain size and internal strains has been studied for *Desmophyllum* and *Favia* corals, for both natural and annealed samples. We fitted each Bragg peak observed in the SR diffraction pattern separately to a pseudo-Voigt profile shape and the observed FWHM (denoted as w) was analyzed as a function of the scattering angle 2θ . The instrumental peak width was estimated by measuring a reference LaB₆ sample. The Bragg peaks observed for all the coral samples are at least three times broader than the instrumental peak width, so the instrumental contribution to the peak width was not subtracted. The results are shown in the form of Williamson–Hall plots in Fig. 6. Note that the different scales in Fig. 6 are related to the different wavelengths used. The straight lines shown in the plots are the result of a linear fit:

$$w^2 \cos^2 \theta = IG + U \sin^2 \theta. \quad (1)$$

One can clearly see that both *Desmophyllum* (Fig. 6a) and *Favia* (Fig. 6b) reveal the same tendency; natural coral samples have much less internal strains than the annealed samples. The obtained values of IG are very close to zero and involve a large statistical error so it is not possible to estimate


Figure 6

Williamson–Hall plot showing the angular dependence of the Bragg peak widths, w , for the natural coral (solid circles) and the coral annealed at 773 K (empty circles). The data for *Desmophyllum*, *Favia* and as-prepared aragonite are shown in the panels (a), (b) and (c), respectively. The lines show a linear plot fitted to the experimental data.

the average grain size from such data. The slope parameter U is related to the internal strain, $\varepsilon \propto U^{1/2}$. The values of the average internal strains were calculated by the method reported by Rodriguez-Carvajal *et al.* (1991). For natural and annealed *Desmophyllum* we obtained $\varepsilon = 0.055$ and 0.120%,

respectively. For natural and annealed *Favia* we obtained $\varepsilon = 0.053$ and 0.106% , respectively. The results for synthetic aragonite (Fig. 6c) differ from those of the biogenic samples. Both as-prepared and annealed synthetic aragonite show similar values of ε , viz. 0.120 and 0.126% , respectively.

4. Discussion

Several remarkable chemo-physical properties of biominerals can be explained by their composite, organo-mineral structures. Mineral units are closely associated with the organic components and this correspondence occurs both at macro- and nanostructural levels of the hierarchical organization (see also Cuif & Dauphin, 2005a,b; Stolarski & Mazur, 2005; Dauphin *et al.*, 2006; Li *et al.*, 2006). There is a growing demand for examination of biominerals *in situ*, under conditions similar to those occurring in nature. Our work shows that it is possible to assess lattice parameters of biogenic aragonite by using entire pieces of the scleractinian coral samples without preliminary pulverization. Such natural coral samples yield narrow Bragg peaks with $\Delta d/d$ values as low as 1×10^{-3} , which allows us to take advantage of the high resolution of the synchrotron beamline.

Biogenic aragonite extracted from two coral skeletons, *Desmophyllum* and *Favia*, shows the same type of anisotropic elongation of the lattice parameters $a/b/c$ as that reported for biogenic aragonite extracted from bivalve, gastropod and cephalopod shells (Pokroy *et al.*, 2004; Pokroy, Fitch, Lee *et al.*, 2006). It still needs to be verified whether the crystal structure in biogenic aragonites is modified by its interactions with organic molecules that are initially present in the biomineralization hydrogel. Regardless of whether this is intercalation of guest molecules or not, our results seem to support the thesis of Pokroy, Fitch, Lee *et al.* (2006) that deformation in the crystal structure of biominerals is a universal phenomenon.

The morphology of the crystallites obtained by annealing is, on the microstructural level, considerably different from that of the biomineral fibers in the natural coral; the original fibers (aragonite mineral phase) disintegrate into grains with average sizes of about $5\text{--}10 \mu\text{m}$ (calcite mineral phase) after annealing (Figs. 1 and 2). Remarkably, the internal strain of the resulting calcite structure is about two times larger than that in the natural aragonite (Fig. 6). This effect is observed despite slow annealing and cooling procedures in which we tried to minimize the internal strains in annealed biominerals. The increase of internal strain in the samples examined here may be related to a decrease of mechanical strength observed by Fricain *et al.* (2002) in the annealed skeleton of *Porita lutea* scleractinian coral. It is not clear at this stage whether the increase of internal strains and also the decrease of mechanical strength of calcite is an intrinsic property of the aragonite/calcite phase transition or a fact that originates from intercalation of the organic molecules into the crystal structure. Recently, Dauphin *et al.* (2006) have shown that some organic components present in the coral skeleton can withstand 773 K thermal treatment and organic molecules may still be present

in the host lattice after thermally induced phase transformation.

We also note that the unit-cell volume and the lattice parameter ratio c/a of the calcite phase obtained from annealed coral samples are considerably different from those of reference geological calcite and annealed synthetic aragonite. Our findings are in agreement with a recent study of calcite biominerals (Pokroy, Fitch, Marin *et al.*, 2006) in which large c/a ratios were reported in natural skeletons of five mollusk species. The c/a ratio observed in our study for annealed *Desmophyllum* and *Favia* (ca 3.423) is located between the high values observed in natural calcite biominerals (ca 3.424–3.425) and values for reference geological calcite (ca 3.420–3.422). Pokroy, Fitch, Marin *et al.* (2006) have also shown that, after annealing at temperatures up to 873 K , the c/a ratio decreases and tends to the value observed in synthetic or geological reference calcite. Pokroy, Fitch, Marin *et al.* (2006) suggested also that intercalated organic molecules influence the crystal structure of calcite. In our paper we suggest that the influence of these intercalated organic molecules affects also the aragonite-to-calcite phase transition.

Finally, our results show that the structural properties of aragonite from biominerals occurring in two ecologically different taxa (shallow-water, colonial, zooxanthellate *Favia* and deep-water, solitary and azooxanthellate *Desmophyllum*) reveal similar anisotropic elongations of the lattice parameters a , b and c . In addition, the internal strain values, cell volume and lattice parameter ratio c/a of the calcite obtained *via* thermal annealing of the biomineral are similar for both corals.

The authors acknowledge the European Synchrotron Radiation Facility (ESRF, Grenoble, France) for provision of synchrotron radiation facilities. Thanks are due to Maciej Kamiński and Izabela Sosnowska (Warsaw University) for fruitful discussions. This is the third publication of the BIOMIMAT (Biominerals, Biomimetics, Biomaterials) initiative, which aims to stimulate interdisciplinary research on the origin, evolution, formation and practical applications of biominerals.

References

- Ajikumar, P. K., Wong, L. G., Subramanyam, G., Lakshminarayanan, R. & Valiyaveetil, S. (2005) *Cryst. Growth Des.* **5**, 1129–1134.
- Caspi, E. N., Pokroy, B., Lee, P. L., Quintana, J. P., Zolotoyabko, E. (2005). *Acta Cryst.* **B61**, 129–132.
- Cuif, J.-P. & Dauphin, Y. (1998). *Palaeontol. Z.* **72**, 257–270.
- Cuif, J.-P. & Dauphin, Y. (2005a). *J. Struct. Biol.* **150**, 319–331.
- Cuif, J.-P. & Dauphin, Y. (2005b). *Biogeosciences*, **2**, 61–73.
- Cuif, J.-P., Dauphin, Y., Berthet, P. & Jegoudez, J. (2004). *Geochem. Geophys. Geosyst.* **5**, doi:10.1029/2004GC000783.
- Cuif, J.-P., Dauphin, Y., Doucet, J., Salome, M. & Susini, J. (2003). *Geochim. Cosmochim. Acta*, **67**, 75–83.
- Cuif, J.-P., Dauphin, Y., Freiwald, A., Gautret, P. & Zibrowius, H. (1999). *Comput. Biochem. Physiol. A*, **123**, 269–278.
- Cuif, J.-P., Dauphin, Y. & Gautret, P. (1997). *Bol. R. Soc. Esp. Hist. Nat. (Sec. Geol.)* **92**, 129–141.
- Currey, J. D. & Kohn, A. J. (1976). *J. Mater. Sci.* **11**, 443–463.

- Dana, J. D. (1846). *Zoophytes. United States Exploring Expedition During the Years 1838–1842, Under the Command of Charles Wilkes*, Vol. 7, pp. 1–740.
- Dauphin, Y. (2001). *Int. J. Biol. Macromol.* **28**, 293–304.
- Dauphin, Y., Cuif, J.-P. & Massard, P. (2006). *Chem. Geol.* **231**, 26–37.
- De Villiers, J. P. R. (1970). *Am. Mineral.* **56**, 758–766.
- Esper, E. J. C. (1794). *Fortsetzungen der Pflanzenthier in Abbildungen nach der Natur mit Farben erleuchtet*, Vol. 1, pp. 1–64.
- Fitch, A. N. (2004). *Res. Natl Inst. Stand. Technol.* **109**, 133–142.
- Fricain, J.-Ch., Souillac, V., Albingre, L. & Lepeticorps, Y. (2002). *Cah. ADF*, **12–13**, 18–23.
- Ganteaume, M., Baumer, A., Lapraz, D., Iacconi, P., Bokilo, J. E., Bernat, M. & Zahra, C. (1990). *Thermochim. Acta*, **170**, 121–137.
- Gautret, P., Cuif, J. P. & Stolarski, J. (2000). *Acta Palaeontol. Pol.* **45**, 107–118.
- Grégoire, Ch. (1967). *Biol. Rev.* **42**, 653–687.
- Jarosch, D. & Heger, G. (1986). *Tscher. Miner. Petrog.* **35**, 127–131.
- Jelinski, L. (1999). *Nanostructure Science and Technology, A Worldwide Study*. <http://itri.loyola.edu/nano/final/>, pp. 113–130.
- Li, X. D., Xu, Z. H. & Wang, R. Z. (2006). *Nano Lett.* **6**, 2301–2304.
- Lucas, A., Mouallem-Bohout, M., Carel, C., Gaudé, J. & Matecki, M. (1999). *J. Solid State Chem.* **146**, 73–78.
- Maslen, E. N., Streltsov, V. A., Streltsova, N. R. & Ishizawa, N. (1995). *Acta Cryst.* **B51**, 929–939.
- Mutvei, H. (1969). *Stockholm Contrib. Geol.* **20**, 1–17.
- Mutvei, H. (1979). *Scan. Electron Microsc.* **2**, 451–462.
- Passe-Coutrin, N., N'Guyen, Ph., Pelmard, R., Ouensaga, A. & Bouchon, C. (1995). *Thermochim. Acta*, **265**, 135–140.
- Pilati, D., Demartin, F. & Gramaccioli, C. M. (1998). *Acta Cryst.* **B54**, 515–523.
- Pokroy, B., Fitch, A. N., Lee, P. L., Quintana, J. P., Caspi, E. N. & Zolotoyabko, E. (2006). *J. Struct. Biol.* **153**, 145–150.
- Pokroy, B., Fitch, A. N., Marin, F., Kapon, M., Adir, N. & Zolotoyabko, E. (2006). *J. Struct. Biol.* **155**, 96–103.
- Pokroy, B., Quintana, J. P., Caspi, E. N., Berner, A. & Zolotoyabko, E. (2004). *Nat. Mater.* **3**, 900–902.
- Rietveld, H. M. (1969). *J. Appl. Cryst.* **2**, 65–71.
- Rodriguez-Carvajal, J. (1993). *Physica B*, **192**, 55–69.
- Rodriguez-Carvajal, J., Fernandez-Diaz, M. T. & Martinez, J. L. (1991). *J. Phys. Condens. Matter*, **3**, 3215–3234.
- Rousseau, M., Lopez, E., Stempflié, P., Brendlé, M., Franke, L., Guette, A., Naslain, R. & Bourrat, X. (2005). *Biomaterials*, **26**, 6254–6262.
- Stolarski, J. (2003). *Acta Paleontol. Pol.* **48**, 497–530.
- Stolarski, J. & Mazur, M. (2005). *Acta Palaeontol. Pol.* **50**, 847–865.
- Vongsavat, V., Winotai, P. & Meejoo, S. (2006). *Nucl. Instrum. Methods Phys. Res. B*, **243**, 167–173.
- Wainwright, S. A. (1963). *Q. J. Microsc. Sci.* **104**, 169–183.
- Waite, J. H. & Andersen, S. O. (1980). *Biol. Bull.* **158**, 164–173.
- Williamson, G. K. & Hall, W. H. (1953). *Acta Metall. Mater.* **1**, 22–31.
- Yoshika, S. & Kitano, Y. (1985). *Geochem. J.* **19**, 245–249.